Naunyn-Schmied Arch Pharmacol (2009) 379:551–564
DOI 10.1007/s00210-009-0401-4

ORIGINAL ARTICLE

Epigallocatechin-3-gallate induced primary cultures of rat hippocampal neurons death linked to calcium overload and oxidative stress

Shu-Ting Yin · Ming-Liang Tang · Hong-Min Deng · Tai-Ran Xing · Ju-Tao Chen · Hui-Li Wang · Di-Yun Ruan

Received: 7 August 2008 / Accepted: 19 January 2009 / Published online: 17 February 2009

Abstract Epigallocatechin-3-gallate (EGCG), a catechin polyphenols component, is the main ingredient of green tea extract. It has been reported that EGCG is a potent antioxidant and beneficial in oxidative stress-related diseases, but others and our previous study showed that EGCG has prooxidant effects at high concentration. Thus, in this study, we tried to examine the possible pathway of EGCG-induced cell death in cultures of rat hippocampal neurons. Our results showed that EGCG caused a rapid elevation of intracellular free calcium levels ($[Ca^{2+}]_i$) in a dose-dependent way. Exposure to EGCG dose- and time-dependently increased the production of reactive oxygen species (ROS) and reduced mitochondrial membrane potential ($\Delta\psi_m$) as well as the Bcl-2/Bax expression ratio. Importantly, acetoxymethyl ester of 5,5′-dimethyl-bis(*o*-aminophenoxy)ethane-*N,N,N′,N′*-tetraacetic acid, ethylene glycol-bis-(2-aminoethyl)-*N,N,N′,N′*-tetraacetic acid, and vitamin E could attenuate EGCG-induced apoptotic responses, including ROS generation, mitochondrial dysfunction, and finally partially prevented EGCG-induced cell death. Furthermore, treatment of hippocampal neurons with EGCG resulted in an elevation of caspase-3 and caspase-9 activities with no significant accompaniment of lactate dehydrogenase release, which provided further evidence that apoptosis was the dominant mode of EGCG-induced cell death in cultures of hippocampal neurons. Taken together, these findings indicated that EGCG induced hippocampal neuron death through the mitochondrion-dependent pathway.

S.-T. Yin · M.-L. Tang · H.-M. Deng · T.-R. Xing · J.-T. Chen · H.-L. Wang · D.-Y. Ruan (✉)
School of Life Science,
University of Science and Technology of China,
Hefei, Anhui 230027, People's Republic of China
e-mail: Ruandy@ustc.edu.cn

Keywords EGCG · Hippocampal neuron · Calcium overload · Oxidative stress · Apoptosis

Abbreviations

Ac-DEVD-*p*NA	Acetyl-Asp-Glu-Val-Asp *p*-nitroanilide
Ac-LEHD-*p*NA	Acetyl-Leu-Glu-His-Asp *p*-nitroanilide
BAPTA-AM	Acetoxymethyl ester of 5,5′-dimethyl-bis(*o*-aminophenoxy)ethane-*N,N,N′,N′*-tetraacetic acid
CNS	Central nervous system
DCF	Dichlorofluorescein
DCFH-DA	2′,7′-Dichlorofluorescein diacetate
DMEM	Dulbecco's modified Eagle's medium
DMSO	Dimethyl sulfoxide
EGCG	Epigallocatechin-3-gallate
EGTA	Ethylene glycol-bis-(2-aminoethyl)-*N,N,N′,N′*-tetraacetic acid
ER	Endoplasmic reticulum
Fluo-3-AM	Fluo-3-acetoxymethyl ester
HEPES	4-(2-hydroxyethyl)-1-201 piperazineethanesulfonic acid
JC-1	5,5′,6,6′-Tetrachloro-1,1′,3,3′-tetraethylbenzimidazolcarbocyanine iodide
LDH	Lactate dehydrogenase
mPT	Mitochondria permeability transition
MTT	3-(4,5-Dimethylthiazol-2-yl)-2, 5-diphenyltetrazolium bromide
PBS	Phosphate-buffered saline
PI	Propidium iodide
*p*NA	*p*-nitroanilide
ROS	Reactive oxygen species
$\Delta\psi_m$	Mitochondrial membrane potential

Introduction

Green tea is used worldwide as a health-promoting beverage. Among the bioactive chemicals in green tea, epigallocatechin-3-gallate (EGCG), the main constituent of the polyphenols, is most abundant and active because of its potent biological effects. Epidemiological cell culture and in vivo studies, including those in humans, have demonstrated that EGCG have antioxidant (Nakagawa and Yokozawa 2002), hepatoprotective (Sai et al. 1998), chemopreventive (Chung et al. 2003), and anticarcinogenic (Lambert and Yang 2003) effects. On the other hand, several studies have indicated genotoxic and carcinogenic potentials of EGCG (Kanadzu et al. 2006; Bandele and Osheroff 2008). A high dose of green tea polyphenols can induce gastrointestinal carcinogenesis (Lambert et al. 2007) and exert acute toxicity in liver cells (Schmidt et al. 2005). However, the cellular and molecular mechanisms mediating these processes are not completely understood and the molecular mechanisms by which EGCG induces cell death have not yet been elucidated.

Calcium ions are central to multiple signal transduction pathways to accomplish a variety of biological functions. The spatial and temporal regulation of intracellular calcium ($[Ca^{2+}]_i$) serves as a modulator of pathways involved in learning and memory, fertilization, proliferation, and development (Berridge et al. 2000). However, high $[Ca^{2+}]_i$ can cause disruption of mitochondrial Ca^{2+} equilibrium, which results in reactive oxygen species (ROS) formation due to the stimulation of electron flux along the electron transport chain (Chacon and Acosta 1991). Under oxidative stress, mitochondrial Ca^{2+} accumulation can switch from physiologically beneficial process to cell death signal (Ermak and Davies 2002).

The brain is especially sensitive to oxidative stress, due to the lipid composition of cell membranes and low levels of antioxidant enzymes (Marttila et al. 1988). Within central nervous system (CNS), the response to oxidative stress has been shown to vary according to the various cellular phenotypes, and it is reported that the antioxidant capacity of neurons is lower than that of glia (Makar et al. 1994) and neurons are more susceptible than glial cells (Cafe et al. 1995). Neurons from the hippocampus, grown in chemically defined medium, provide a convenient in vitro method for studying biochemical changes following EGCG exposure.

Until now, the majority of studies both in vivo and in vitro have focused to elucidate the antioxidant effects of EGCG after the treatment of cells with pro-oxidants. In our previous study, we have found that EGCG treatment for 24 and 48 h inhibit the MTT reduction, an indicator of cell viability, of primary hippocampal cultures at concentrations above 100 μM (Yin et al. 2008). Therefore, in this study, we examined the effects of EGCG in oxidative stress of cultures of hippocampal neurons. By using a series of concentrations up to 100 μM in a time-dependent way, $[Ca^{2+}]_i$, ROS production, apoptotic protein, mitochondrial membrane potential ($\Delta\psi_m$), and cell morphological changes in cultures of hippocampal neurons have been evaluated. The $[Ca^{2+}]_i$ was increased significantly immediately after EGCG exposure, and the calcium overload was then followed by massive production of ROS, $\Delta\psi_m$ alterations, a reduction of Bcl-2 expression and an increase of Bax expression in a temporal sequence. Our results indicated that EGCG acts at least in part as a weak pro-oxidant in hippocampal neurons and these detrimental effects should be carefully studied before considering the use of green tea catechins as cancer chemopreventive agents.

Materials and methods

Chemicals

EGCG was obtained from Leshan Yujia Tea Science and Technology Development. Dulbecco's modified Eagle's medium (DMEM), fetal bovine serum, neurobasal medium, and B-27 were obtained from Gibco, Invitrogen Corporation, Carlsbad, CA, USA. Fluo-3-acetoxymethyl ester (Fluo-3-AM) was purchased from Dojindo Laboratory (Kumamoto, Japan). Acetoxymethyl ester of 5,5′-dimethyl-bis(*o*-aminophenoxy)ethane-*N,N,N′,N′*-tetraacetic acid (BAPTA-AM), cytosine arabinoside, 2′,7′-dichlorofluorenscein diacetate (DCFH-DA), ethylene glycol-bis-(2-aminoethyl)-*N,N,N′,N′*-tetraacetic acid (EGTA), pluronic F-127, poly-L-lysine, thapsigargin, and vitamin E were purchased from Sigma Chemical (St. Louis, MO, USA). Hoechst 33342 kit was from Immunotech (Marseille, France). 5,5′,6,6′-tetrachloro-1,1′,3,3′-tetraethylbenzimidazolo-carbocyanine iodide (JC-1) was from Molecular Probes, Eugene, OR, USA. Caspase-3 and caspase-9 activity assay kits were provided by Beyotime Institute of Biotechnology (Haimen, China). Lactate dehydrogenase (LDH) activity kit and total protein quantification kit (Coomassie Brilliant Blue) were provided by Nanjing Jiancheng Bioengineering Institute (Nanjing, China). Antibodies for Bcl-2, Bax, and β-actin were purchased from Santa Cruz Biotechnology (Santa Cruz, CA, USA). Enhanced chemiluminescence (ECL) reagents were from Amersham International (Amersham, Arlington, Heights, IL, USA). Twelve-well and 24-well plates were purchased from Corning Costar, Cambridge, MA, USA. All other chemicals used were of the highest grade available.

Primary culture of hippocampal neurons

Zero-day-old Wistar rat pups were decapitated and hippocampal neurons were isolated and cultured according to published procedures (Sunanda et al. 1998). Briefly, the

hippocampi were carefully collected, gently dispersed in culture medium, and triturated with a pipette. Then, neurons were seeded onto poly-L-lysine (10 μg/ml)-coated 12-well plates (Corning Costar) for Western blots or 8×8 mm square glass coverslips in 24-well plates for immunofluorescence studies. Cells were seeded at a density of 2×10^5/ml in DMEM supplemented with 10% fetal bovine serum (Gibco, USA), 0.11% $NaHCO_3$, 0.11% 4-(2-hydroxyethyl)-1-piperazineethanesulfonic acid (HEPES), 0.11% penicillin (10 IU/ml), and streptomycin (0.11%). Cultures were maintained at 37°C in a humidified atmosphere of 95% air/5% CO_2. Cytosine arabinoside (10 μM; Sigma, USA) was added to the culture medium 18–24 h after plating in order to arrest the growth of non-neuronal cells. The medium was replaced at an interval of every 2 days with a maintenance medium containing neurobasal media and 5% B-27 supplement (Gibco, USA). After 7 days of culture in vitro, successful cultures of neurons were selected for further studies.

Before use, EGCG was dissolved in H_2O to generated 0.1, 1, 5, 10, and 20 mM of 100× stock solutions. In some experiments, the intracellular calcium chelator BAPTA-AM at 5 mM in dimethyl sulfoxide (DMSO) solution (final concentration 5 μM) or vitamin E at 20 mM in DMSO solution (final concentration 20 μM), was introduced 1 h before EGCG exposure. It was checked that DMSO at these concentrations had no effect on hippocampal neurons. The extracellular calcium chelator EGTA at 5 mM was added directly to the culture medium 1 h before EGCG exposure.

Measurement of intracellular free calcium levels

The free $[Ca^{2+}]_i$ in hippocampal neurons was quantified by fluorescence ratio imaging of the Ca^{2+} indicator dye Fluo-3-AM using the methods detailed previously (Mattson et al. 1995). Briefly, primary cultures of hippocampal neurons were washed with the standard external solution containing (in mM): 150 NaCl, 5 KCl, 2 $CaCl_2$, 1 $MgCl_2$, 10 HEPES, and 10 D-glucose and buffered to pH7.3. The standard external solution was continuously bubbled with carbogen (95% O_2/5% CO_2). Cells were loaded with 5 μM Fluo-3-AM and pluronic F-127 (Sigma, 0.004% (*w*/*v*) final) in the standard external solutions for 45 min at 37°C in dark. Endogenous esterases converted non-fluorescent Fluo-3-AM into fluorescent Fluo-3. The cells were then washed twice with the external solutions and incubated for another 20 min at 37°C before imaging. Images were obtained using a scanning confocal microscope (Zeiss LSM510, Carl Zeiss Microimaging, Thornwood, NY, USA). Different concentrations of EGCG (1, 10, 50, 100, and 200 μM final) were added to the standard external solution by dilution from 100× stocks. For calcium-free groups, calcium was excluded from the external solutions, while 40 μM EGTA was added to ensure calcium-free environment. For the thapsigargin group, cultures were incubated with 2 μM thapsigargin for at least 40 min before imaging to deplete endoplasmic reticulum (ER) calcium stores (Doutheil et al. 1999).

To measure the change of cytoplasmic calcium levels under EGCG exposure, camera gain was adjusted to give baseline maximal fluorescence levels of 40–100 (arbitrary units) of a maximal 8-bit signal output of 256 and time-lapse sequences were recorded at a scanning rate of each 60 s. The dye was excited with an argon laser at 488 nm and the emitted fluorescence was collected at 510–550 nm. Cell fluorescence during the 5 min baseline period was F_0. Fluorescence measurements for each cell (F) were normalized to the average fluorescence intensity. Region of indexes (ROIs) were defined in the first image, and the normalized fluorescence changes $(F-F_0)/F_0$, that is $\Delta F/F_0$ (in %), were measured throughout the image sequence. All settings of the scanning system and the complete data acquisition were controlled and collected by the Zeiss software. The average $[Ca^{2+}]_i$ in ten neuronal cell bodies/microscope field were quantified in three to four separate cultures per treatment condition.

Determination of ROS production

The dye DCFH-DA was chosen to follow ROS production in cultures of neurons by measuring the increase in fluorescence-associated oxidation of dichlorodihydrofluorescein (DCFH) to dichlorofluorescein (DCF; Lin et al. 2007). After treated with 10, 50, and 100 μM EGCG at 37°C for 1, 2, 4, 8, or 12 h, hippocampal neurons cultured on 8×8 mm square glass coverslips were rinsed with ice-cold phosphate-buffered saline (PBS) and then incubated in 10 μM DCFH-DA (Sigma, USA) for 15 min at 37°C in the dark. Fluorescence was measured using confocal microscope (Zeiss LSM510) at excitation and emission wavelengths of 495 and 535 nm for DCF fluorescence. In average, ten neuronal cell bodies/microscope field were quantified in three to four separate cultures per treatment condition. The software available with the Zeiss confocal microscope was used to demonstrate the changes in the DCF fluorescence intensity.

Analysis of mitochondrial membrane potential ($\Delta\psi_m$)

Following EGCG treatments, hippocampal neurons were stained with the cationic dye, JC-1, as previously described (Reyes-Martin et al. 2007) to visualize the state of mitochondrial membrane potential. Briefly, the uptake of mitochondrion-selective dye is dependent on the potential across the mitochondrial inner membrane. In mitochondria, JC-1 exists as a green fluorescent monomer at low (depolarized) membrane potentials, while at higher (hyperpolarized) potentials, JC-1 forms orange-red fluorescent J-aggregates. Thus, the dual emission of this dye can be used as a measure of mitochondrial membrane potential (Choi et al. 2002).

JC-1 was stocked as 1 mg/ml DMSO solution and freshly diluted with culture medium. Hippocampal neurons cultured on 8×8 mm square glass coverslips, after treated with 100 μM EGCG at 37°C for 1, 2, 4, 8, or 12 h, were then incubated with the filtered JC-1-containing (10 μg/ml) culture medium for 20 min at 37°C in the dark. Following incubation, cells were rinsed twice with PBS and images were obtained using a confocal microscope (Zeiss LSM510) excited at 488 nm (for JC-1) and set to simultaneously detect green emission (510–525 nm) and red emission (590 nm) channels. In each experimental condition, the ratio of red/green fluorescent signal was calculated in 40 randomly selected cells by measuring the average intensities of the emitted fluorescence using the software available with the Zeiss confocal microscope.

Western blotting

After treated with 100 μM EGCG for 4 or 12 h, neurons were washed twice with PBS and proteins were solubilized in the lysis buffer (500 mM Tris–HCl, pH7.4, 150 mM NaCl, 5 mM EDTA, 1 mM benzamiden, 1 μg/ml trypsin inhibitor) containing a cocktail of protease inhibitor. Lysates were incubated for 30 min at 4°C, centrifuged at 12,000×*g* for 20 min. An equivalent amount of protein extracts (20 μg) was electrophoresed on 12% SDS-polyacrylamide gels. The proteins were then electrotransferred to polyvinylidene lifluoride membranes (Millipore Corporation, Bedford, MA, USA) and probed with individual primary antibodies. Detection of each protein was carried out with an ECL Western blotting kit (Amersham, Arlington Heights, IL, USA) according to the manufacturer's instructions. Bands representing β-actin, Bax, and Bcl-2 were determined to be 42, 21, and 26 kDa, respectively. Samples of each group were independently separated three times and the films were scanned with a laser scanner. Quantification of the signal intensity was performed with Scion image beta 4.0.2 analysis software. Mean optical density was measured densitometrically and normalized to housekeeping β-actin protein.

Caspase-3 and caspase-9 activity assay

Caspase-3 and caspase-9 activity were determined by a colorimetric assay based on the ability of caspase-3 and caspase-9 to change acetyl-Asp-Glu-Val-Asp *p*-nitroanilide (Ac-DEVD-*p*NA) and acetyl-Leu-Glu-His-Asp *p*-nitroanilide (Ac-LEHD-*p*NA) into a yellow formazan product *p*-nitroanilide (*p*NA), respectively. An increase in absorbance at 405 nm was used to quantify the activation of caspase activity. After 12 h exposure to 100 μM EGCG, cultures of hippocampal neurons from 12-well plates were collected and rinsed with ice-cold PBS, and then lysed by lysis buffer (50 μl) for 15 min on ice. Cell lysates were centrifuged at 16,000×*g* for 10 min at 4°C, the supernatants were collected, and protein concentration was determined by the total protein quantification kit (Nanjing Jiancheng Bioengineering Institute, Nanjing, China). Approximately 20 μg of total protein was added to the reaction buffer containing Ac-DEVD-*p*NA (2 mM) and Ac-LEHD-*p*NA (2 mM) and incubated for 2 h at 37°C), and the absorbance of yellow *p*NA cleavaged from its corresponding precursors were measured with an enzyme-linked immunosorbent assay (ELISA) reader at 405 nm. The caspase activity, normalized for total proteins of cell lysates, was then expressed as fold of the baseline caspase activity of control neurons.

LDH release

LDH activity in the medium was measured using a LDH assay kit (Nanjing Jiancheng Bioengineering Institute, Nanjing, China). A colorimetric assay was applied, according to which the amount of formazan salt, formed after conversion of lactate to pyruvate and then by reduction of tetrazolium salt, is proportional to LDH activity in the sample. After a 12-h exposure to 100 μM EGCG, cell-free culture supernatants were collected from each well and incubated with the appropriate reagent mixture according to the instructions at 37°C for 30 min. The reaction was stopped by adding five volumes of 0.1 M NaOH, and absorbance was then measured at 440 nm with an ELISA reader. Control lyses were obtained by using supernatants of untreated cells and cells treated with 0.1% Triton-X 100. Each reading was subtracted from the reading obtained in medium containing drugs without cells in order to avoid any interference of the drugs with the reagents in the LDH detection kit. Data were normalized to the activity of LDH released from cells (100%) and expressed as percentage of the control.

Assessment of apoptosis and morphological analysis

After exposing hippocampal neurons to 100 μM EGCG for 1, 2, 4, 8, or 12 h, cell morphology and apoptosis were studied. For primary viability assessment, cells were loaded for 20 minutes with 10 μg/ml of Hoechst 33342 and 1 μg/ml of PI, respectively, and then visualized using a fluorescence microscope (Olympus BX60). Hoechst 33342 is a blue fluorescent probe that stains the nuclei. In apoptotic cells, chromatin condensation occurs, and apoptotic cells can thus be identified as those with condensed and more intensively stained chromatin. Sample fields with approximately 100 cells were randomly selected and evaluated per sample and those cells were scored as either "intact" (normal appearance of dark-blue Hoechst 33342-stained nucleus as well as absence of a red PI staining); "apoptotic" (distinctive condensed and

intensively blue-stained nuclei but without PI-staining); and/or "PI positive" (red PI-staining; late apoptotic cells). The number of intact, apoptotic, and/or PI positive cells was expressed as a percentage of the total number of nuclei counted (cells in five to ten random fields/culture were scored, and counts were made in at least four separate cultures per treatment condition).

Data analysis

The DCF and JC-1 red/green fluorescence ratio was normalized to the control ratio. Data were analyzed with Origin 7.5 (Origin Lab, MA, USA). All values are given as the mean±SEM. One-way ANOVA was performed to determine whether there were significant differences followed by Bonferroni test as post hoc analysis; $p<0.05$ indicated a significant difference.

Results

EGCG induced elevation of intracellular calcium levels via internal calcium release as well as extracellular calcium influx

To examine whether the $[Ca^{2+}]_i$ change was involved in oxidative stress induced by EGCG, we tested the $[Ca^{2+}]_i$ using the Ca^{2+}-sensitive fluorescent indicator Fluo-3. From the results, we found that 100 μM EGCG induced large elevations of $[Ca^{2+}]_i$ in cultures of hippocampal neurons as the Fluo-3 fluorescence ratio increased from basal to 153±10% ($n=20$) and reach a plateau during the next 10 min (Fig. 1G). Moreover, EGCG increased $[Ca^{2+}]_i$ in a concentration-dependent manner from 10 to 200 μM (Fig. 1A–F) while it did not induce elevation of $[Ca^{2+}]_i$ at very low concentration (1 μM; Fig. 1H).

Since the EGCG-induced rise of cytosolic free Ca^{2+} could be due to extracellular calcium influx or internal calcium release, we next used the calcium-free external solutions and 2 μM thapsigargin pre-incubated external solutions to investigate the putative mechanism underlying the rise in cytoplasmic calcium observed after EGCG exposure (Fig. 2A–F). Figure 2G showed that 100 μM EGCG application could elevate the Fluo-3 fluorescence ratio from basal to 139±4.6% in the calcium-free group ($p<0.01$ vs. control, $n=20$), while Fig. 2H showed that 100 μM EGCG application could also induce a significant but smaller elevation on the Fluo-3 fluorescence ratio from basal to 122±9.1% in the thapsigargin group ($p<0.01$ vs. control, $n=20$). When calcium-free solutions were pre-incubated with 2 μM thapsigargin, acute application of 100 μM EGCG failed to elevate the Fluo-3 fluorescence ratio ($p>0.05$ vs. control, $n=20$; Fig. 2I). These data indicated that EGCG affected calcium release process both from extracellular calcium influx and internal calcium release. The extents of elevation of intracellular calcium levels induced by acute application of 100 μM EGCG in standard external solutions, calcium-free external solutions, thapsigargin-pre-incubated external solutions, and thapsigargin-pre-incubated calcium-free external solutions were expressed in Fig. 2J.

EGCG induced ROS accumulation in hippocampal neurons

Increased intracellular levels of calcium have been markedly associated with formation of ROS and increasing intracellular ROS may lead to stress and resultant induction of apoptosis (Nicotera et al. 1994). As EGCG induced large elevation of $[Ca^{2+}]_i$, we next addressed the question of ROS involvement in cultures of hippocampal neurons during EGCG exposure. With this purpose, the cultures of hippocampal neurons were incubated with the membrane permeable probe DCFH-DA. Inside the cells, the oxidation of DCFH to fluorescent DCF resulted in high cellular fluorescence intensities (Fig. 3A).

ROS concentrations significantly increased in the hippocampal neurons in a time- and dose-dependent manner of EGCG treatment (Fig. 3B). ROS concentrations increased with time and reached the highest level after 12 hours with exposure to 10 (146±6% of control), 50 (247±15% of control), and 100 μM EGCG (427±17% of control) from 100±5% of control at the beginning of the trial. The maximal response of ROS concentrations was observed at the highest dose of EGCG tested (100 μM). Meanwhile, there was no significant increase of intracellular ROS in control cells within 12 h. These data indicated that EGCG could induce the increase of intracellular ROS significantly within a short time and the increase of intracellular ROS would maintain high levels for at least 12 h. The elevation of ROS may initiate the intracellular response.

Inhibitory effect of BAPTA-AM, EGTA, and vitamin E on EGCG-induced increase in intracellular ROS production

To further demonstrate the cause-and-effect relationship between elevated $[Ca^{2+}]_i$ levels and EGCG-induced ROS production, we investigated the effects of the extracellular trapping compound EGTA and the intracellular calcium trapping drug BAPTA-AM on ROS production induced by EGCG. Hippocampal neurons were pretreated with 5 μM BAPTA-AM or 5 mM EGTA for 1 h and then treated with or without 10, 50, or 100 μM EGCG for 12 h. As shown in Fig. 3C, both BAPTA-AM and EGTA pretreatment significantly inhibited EGCG-induced ROS production in all EGCG-treated groups ($p<0.01$).

We next pre-incubated the hippocampal neurons with 20 μM vitamin E for 1 h and then treated with or without 10,

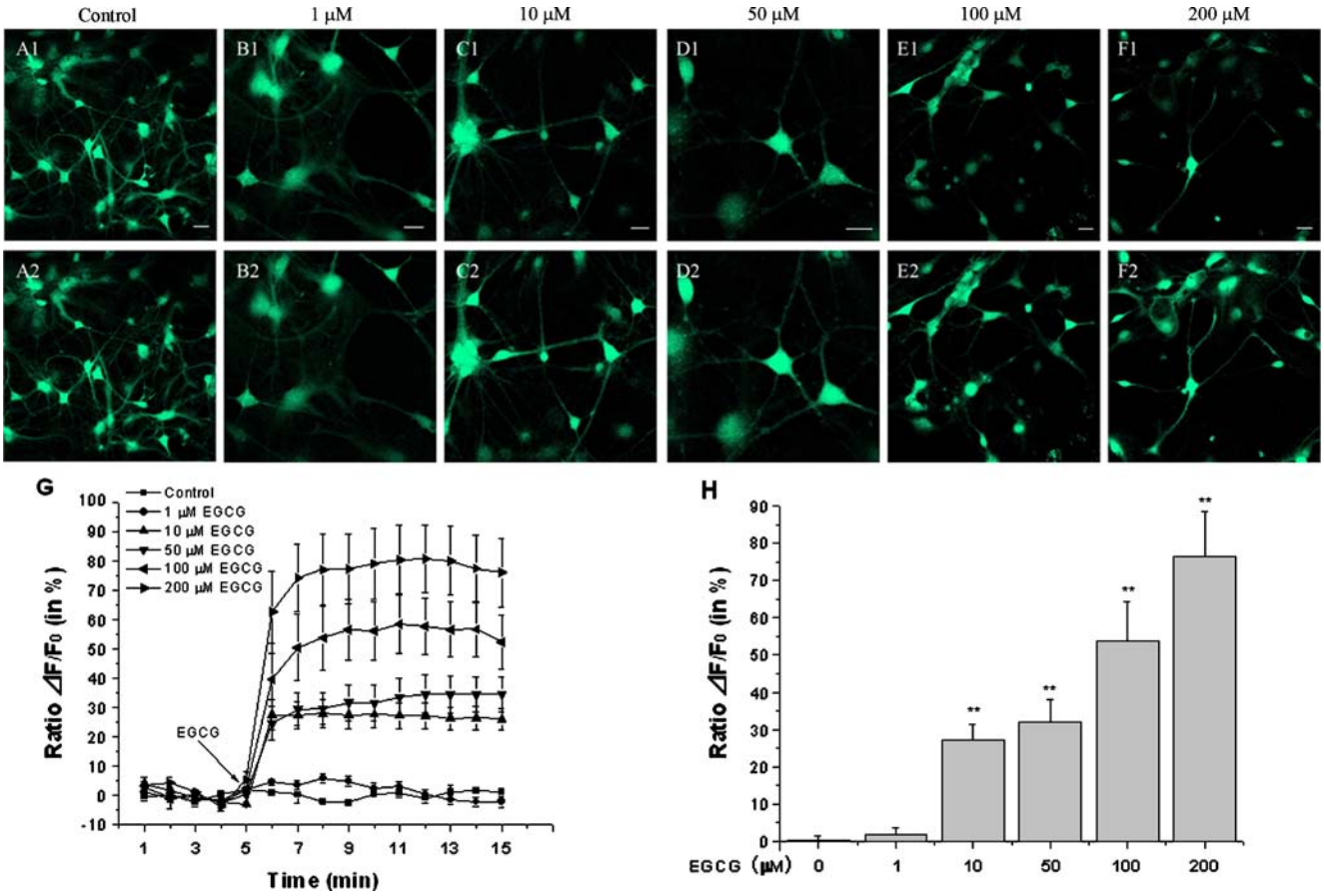

Fig. 1 EGCG induced increases of intracellular calcium levels in hippocampal neurons. Hippocampal cultures were exposed to different concentrations of EGCG and levels of $[Ca^{2+}]_i$ in neurons were quantified by fluorescence ratio imaging of the dye Fluo-3. Cells were exposed to *A* control, *B* 1 μM EGCG, *C* 10 μM EGCG, *D* 50 μM EGCG, *E* 100 μM EGCG, or *F* 200 μM EGCG. In each experiment, the images were obtained under calcium fluorescence before EGCG exposure (*row 1*), 10 min after under fluorescence for EGCG exposure (see "Materials and methods"; *row 2*). *G* Traces showed the mean± SEM of calcium fluorescence ratios ($\Delta F/F_0$) before and after EGCG exposure. *H* Histogram showing mean±SEM of calcium fluorescence ratios ($\Delta F/F_0$) before and after EGCG exposure. $^{**}p<0.01$ compared to corresponding value in control cultures. One-way ANOVA with the Bonferroni post hoc test was used for statistical analysis. All the images are representative of at least three independent experiments with similar results. Scale bar in confocal micrographs, 10 μm

50, or 100 μM EGCG for 12 h. Under vitamin E pretreatment, the EGCG-induced intracellular generation of ROS was, as shown in Fig. 3C, markedly inhibited ($p<0.01$). Vitamin E by itself had no significant effect on ROS production.

These results indicated that calcium overload is involved in the increase of ROS production induced by EGCG exposure.

EGCG induced a decrease in mitochondrial membrane potential in cultures of hippocampal neurons

As increased cytoplasmic levels of calcium and enhanced ROS production are known to secondarily alter mitochondrial homeostasis, we next determined whether EGCG modified mitochondrial membrane potential. To better focus the research towards the effects of EGCG on hippocampal neurons, the subsequent studies were limited to 100 μM as the exposure concentration, which was also a concentration used widely in other studies (Park et al. 2006; Hwang et al. 2007).

Loss of mitochondrial membrane potential ($\Delta\psi_m$) is a sensitive indicator of mitochondrial damage caused by several toxic triggers, and therefore, we performed a time-course assessment of $\Delta\psi_m$ using confocal microscope and a specific and sensitive fluorescent dye, JC-1. Normal hippocampal neurons stained with JC-1 emitted mitochondrial orange-red fluorescence with little green fluorescence (Fig. 4A). Moreover, the mitochondrial fluorescence was shifted to the green by exposure to EGCG, which depolarized the mitochondrial membrane, and this shift happened after 4 h of exposure to EGCG (Fig. 4B). These findings provided potent evidence that a decrease in $\Delta\psi_m$ is involved in EGCG-induced cytotoxicity in hippocampal neurons.

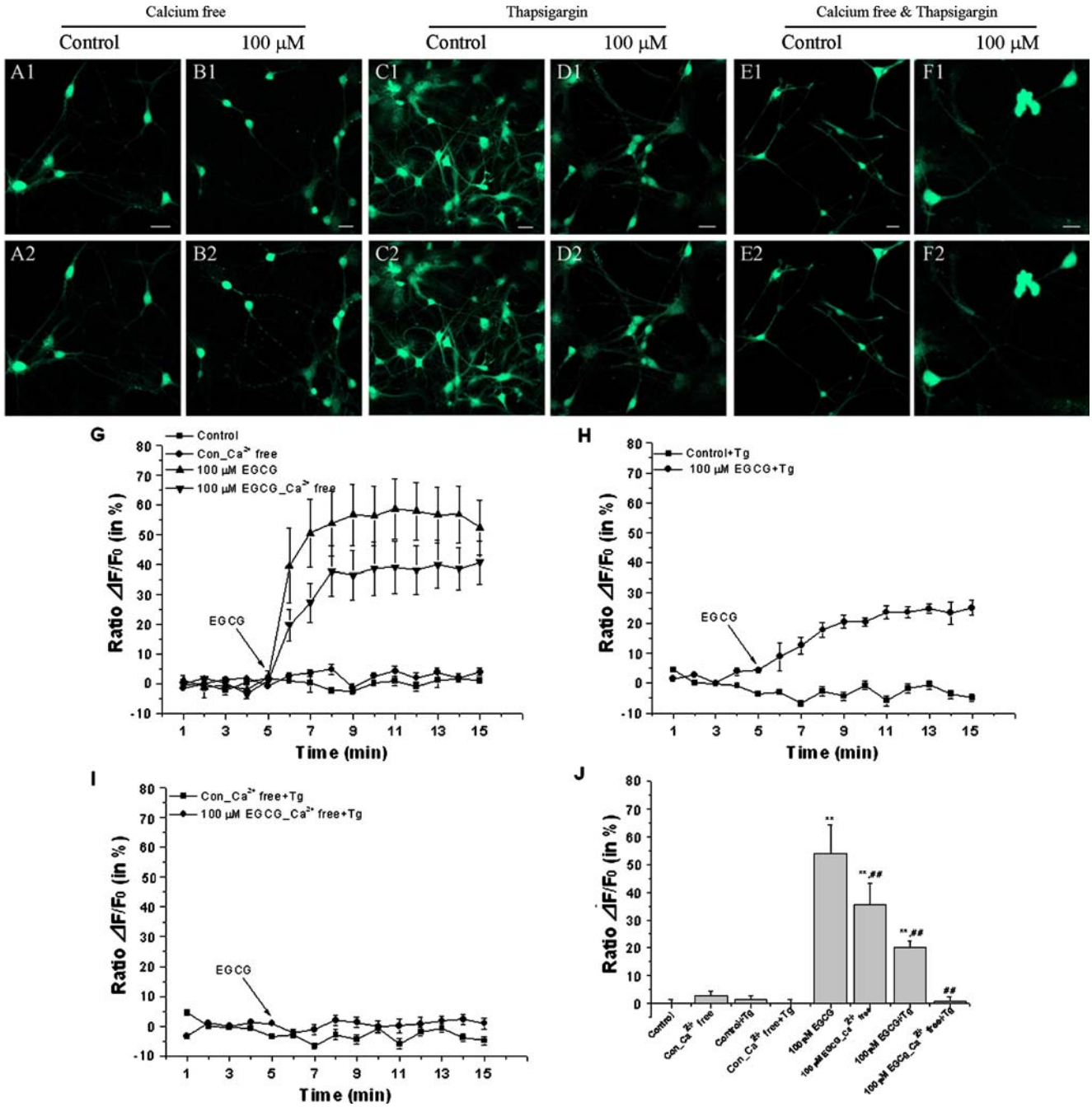

Fig. 2 Hippocampal neurons were loaded with Fluo-3 and calcium levels were expressed as Fluo-3 fluorescence ratios. In each experiment, the images (*A* (control) and *B* (calcium-free); *C* (control) and *D* (thapsigargin); *E* (control) and *F* (calcium-free and thapsigargin)) were obtained before EGCG exposure (*row 1*) and 10 min after 100 μM EGCG exposure (*row 2*). *G* Traces showed the mean±SEM of calcium fluorescence ratios ($\Delta F/F_0$) before and after 100 μM EGCG exposure in normal and calcium-free extracellular fluid. Incubating hippocampal neurons in calcium-free extracellular fluid exposed to 100 μM EGCG caused a decrease in cytoplasmic calcium level but still remained at a level of 139±4.6% of basal. It means that extracellular Ca^{2+} removal does not prevent EGCG-induced increase of intracellular calcium concentrations. *B* Traces showed the mean± SEM of calcium fluorescence ratios ($\Delta F/F_0$) before and after 100 μM EGCG exposure in extracellular fluid exposed to thapsigargin. *I* Thapsigargin exposure of cells in calcium-free extracellular fluid did not induce a rise in cytoplasmic calcium activity indicating that ER calcium stores were depleted. *J* Histogram showing mean±SEM of calcium fluorescence ratios ($\Delta F/F_0$) before and after 100 μM EGCG exposure in various conditions. $^{**}p<0.01$ vs. control group; $\#\#p<0.01$ vs. 100 μM EGCG-exposed group; one-way ANOVA with the Bonferroni post hoc test was used for statistical analysis. All the images are representative of at least three independent experiments with similar results. Scale bar in confocal micrographs, 10 μm

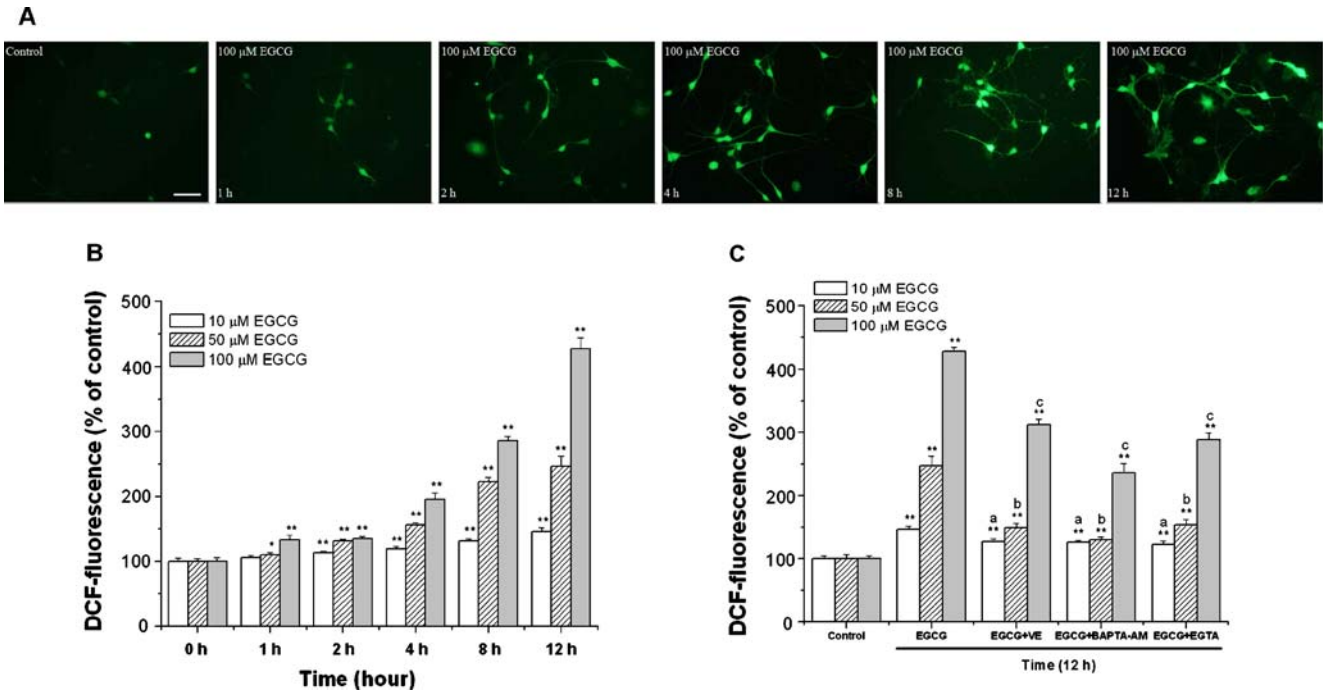

Fig. 3 **A** Representative photographs showing the effect of 100 μM EGCG-induced ROS production in hippocampal neurons after 1, 2, 4, 8, or 12 h. **B** Effect of EGCG exposure on the ROS production in cultures of hippocampal neurons at different concentrations. Hippocampal neurons were treated with 0 (control), 10, 50, or 100 μM EGCG for 1, 2, 4, 8, or 12 h, followed by incubation with 10 μM DCFH-DA for 15 min. Fluorescence was measured at excitation and emission wavelengths of 495 and 535 nm for DCF fluorescence. The results were quantitatively analyzed for changes in fluorescence intensities within cells using the Zeiss LSM software and expressed as percent units of DCF fluorescence of the control. **C** Protective effects of 20 μM vitamin E, 5 μM BAPTA-AM, and 5 mM EGTA on 10, 50, or 100 μM EGCG-induced ROS production. In each experimental condition, the DCF fluorescence was calculated in 30 randomly selected cells. Data are expressed as the mean±SEM of triplicate determinations of four distinct experiments. *$p<0.05$, **$p<0.01$ vs. control group. "a" $p<0.01$ vs. 10 μM EGCG-treated group, "b" $p<0.01$ vs. 50 μM EGCG-treated group, and "c" $p<0.01$ vs. 100 μM EGCG-treated group. One-way ANOVA with the Bonferroni post hoc test was used for statistical analysis. Scale bar in graphs, 20 μm

Inhibitory effect of BAPTA-AM, EGTA, and vitamin E on EGCG-induced loss of $\Delta\psi_m$

To verify the role of $[Ca^{2+}]_i$ as a key second messenger, hippocampal neurons were pre-loaded with 5 μM BAPTA-AM and 5 mM EGTA for 1 h. The results presented in Fig. 4C demonstrate that BAPTA-AM and EGTA pretreatment suppressed EGCG-induced mitochondrial impairment. BAPTA-AM and EGTA were able to prevent decrease in $\Delta\psi_m$ induced by EGCG, indicating the importance of normal Ca^{2+} signaling on mitochondrial function.

In order to study the relationship between EGCG-induced ROS generation and loss of $\Delta\psi_m$, the effect of vitamin E on EGCG-induced loss of $\Delta\psi_m$ was tested. Figure 4C showed that the decrease in the red/green fluorescent intensity ratio of JC-1 significantly increased in the presence of 20 μM vitamin E as assessed at 4 h in cultures treated with 100 μm EGCG ($p<0.01$).

Effect of EGCG on the expression of anti- and pro-apoptotic proteins

As we know, the Bcl-2 family of proteins plays a crucial role in the regulation of apoptosis in the nervous system (Akhtar et al. 2004), we next examined whether or not EGCG has any effect on the expression of pro-apoptotic protein Bax as well as anti-apoptotic protein, Bcl-2, in hippocampal neuron cultures. Using western blot analysis (Fig. 5a), we found that in hippocampal neurons, the level of Bax protein expression increased significantly (Fig. 5b) after EGCG exposure in comparison to the control cultures, while the level of Bcl-2 decreased upon EGCG treatment (Fig. 5c) thereby resulting in a decrease in Bcl-2/Bax ratio (Fig. 5d). These results suggested that EGCG treatment disrupted the balance between positive and negative regulators of apoptosis.

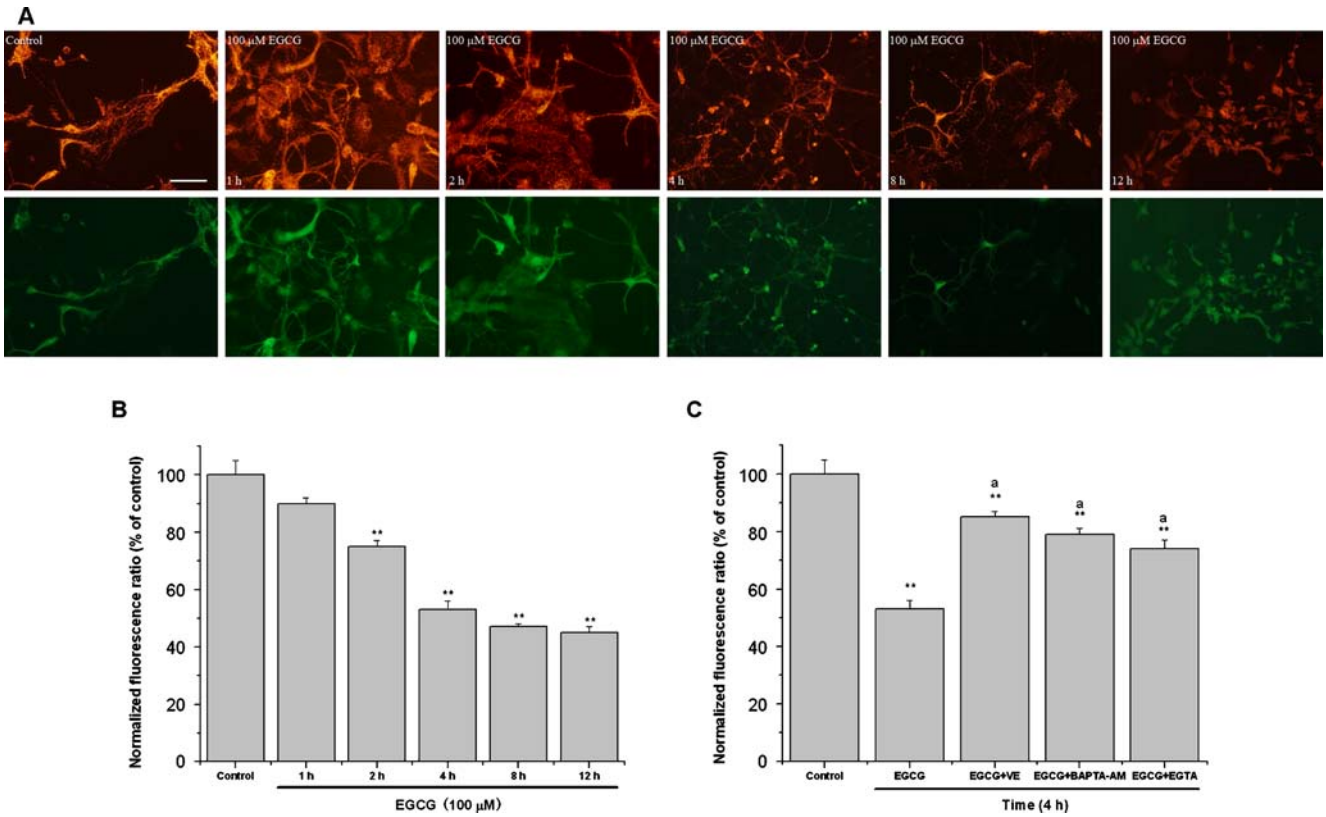

Fig. 4 **A** Representative photographs of 100 μM EGCG-induced mitochondrial membrane depolarization in hippocampal neurons after 1, 2, 4, 8, or 12 h (from *left to right* are control, 100 μM EGCG exposed for 1, 2, 4, 8, or 12 h, respectively). Cultures were treated with 100 μM EGCG after various time intervals stained with 10 μg/ml JC-1, a $\Delta\psi_m$ sensitive dye, for 20 min. Note that at high membrane potential, JC-1 forms red fluorescent "J-aggregates", while at lower membrane potential this dye emits a green fluorescence. **B** Quantitative analysis of red/green fluorescent intensity ratio in the indicated experimental conditions. **C** Protective effect of 20 μM vitamin E, 5 μM BAPTA-AM, and 5 mM EGTA against mitochondrial membrane depolarization induced by 100 μM EGCG. In each experimental condition, the ratio of red/green fluorescent signal was calculated in 40 randomly selected cells by measuring the average intensities of the emitted fluorescence using the software available with the Zeiss confocal microscope. $^{**}p<0.01$, vs. control group and "a" $p<0.01$ vs. 100 μM EGCG-treated group. One-way ANOVA with the Bonferroni post hoc test was used for statistical analysis. Scale bar in confocal micrographs, 20 μm

EGCG induced caspase-9 and caspase-3 activation with no LDH release

Caspases, a group of cysteine proteases, have been demonstrated to play a pivotal role in the induction of apoptosis. To further determine whether the apoptosis induced by EGCG in cultures of hippocampal neurons is mediated by the caspase route and whether this pathway is via mitochondrial alterations, the caspase-9 and caspase-3 activities were checked. After a 12-h exposure, 100 μM EGCG induced caspase-9 activation (115±1.8% of control value) as well as caspase-3 activation (121±2.3% of control value; Fig. 6A). On the other hand, no significant elevation in the level of LDH release was observed within the same duration ($p>0.05$ vs. control) (Fig. 6B), suggesting that 100 μM EGCG induced cultures of hippocampal neurons death mainly via apoptosis rather than necrosis.

Characterization of EGCG-induced cell death in hippocampal neurons

The morphological changes of apoptotic hippocampal neurons induced by EGCG were observed by DNA binding fluorochrome Hoechst 33342 staining. As shown in Fig. 7a, after hippocampal neurons were exposed to 100 μM EGCG for 1, 2, 4, 8, or 12 h, the cells obviously exhibited apoptotic nuclear condensation. After incubation with 100 μM EGCG, the number of apoptotic neurons significantly increased to 20.1±1.4% with 7.2±0.7% of late apoptosis (Hoechst positive/PI positive) at 2 h, and increased further to 39.6± 1.6% with 17.8±2.9% of late apoptosis at 12 h (Fig. 7b). The apoptotic cells ("Hoechst positive") accounted for less than 7% of total cells while hippocampal neurons were cultured alone for 12 h.

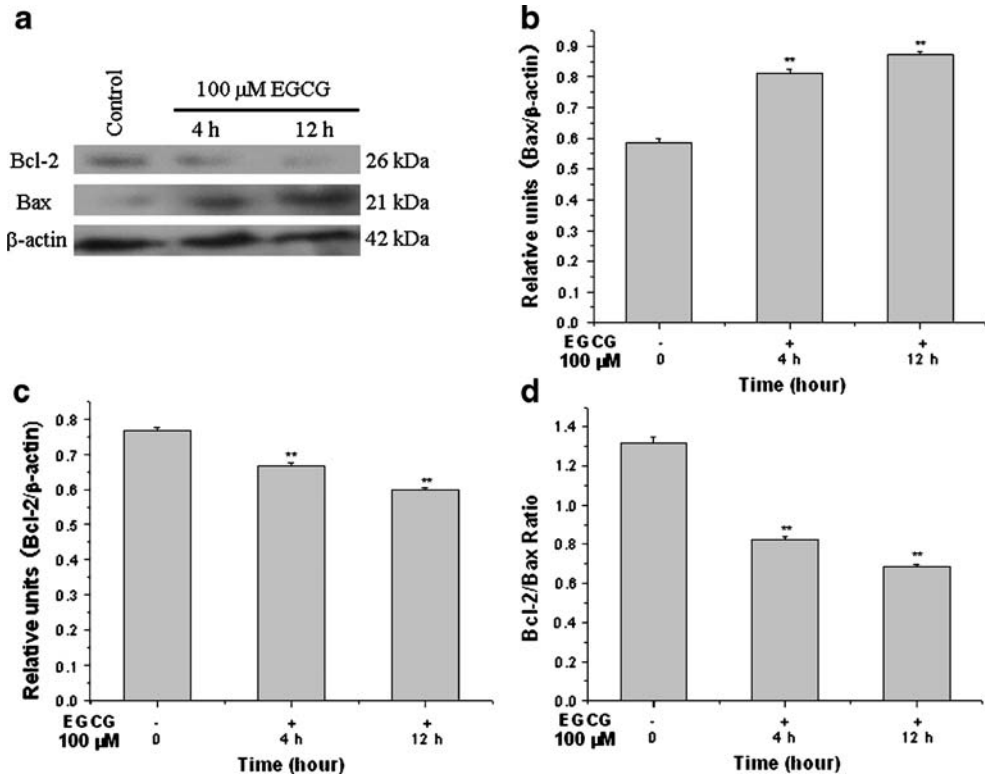

Fig. 5 Effect of EGCG upon the expression of Bcl-2 and Bax in the hippocampal neurons. Cell lysates of hippocampal neurons from control and 100 μM EGCG-treated for 4 and 12 h were subjected to Western blot analysis using anti-Bax, anti-Bcl-2, and anti-β-actin antibodies and visualized with chemiluminescence. A representative autoradiograph is shown (**a**). The *bar diagram* shows the densitometric analyses of the immunoblots of Bax (**b**) and Bcl-2 proteins (**c**). Each point on the *bar diagram* represents the mean density of the apoptotic proteins compared to the control (β-actin). Note the increase in the levels of the Bax (**b**) and concomitant decrease in the levels of Bcl-2 (**c**) following EGCG exposure. **d** The Bcl-2 to Bax ratio determined by densitometer was plotted. Data are expressed as the mean±SEM, *$p<0.05$ vs. control group; **$p<0.01$ vs. control group. One-way ANOVA with the Bonferroni post hoc test was used for statistical analysis

Inhibitory effect of BAPTA-AM, EGTA, and vitamin E on EGCG-induced cell death

To determine the role of calcium and oxidative stress in the regulation of EGCG-induced cell death, hippocampal neurons were incubated with 100 μM EGCG in the absence or presence of BAPTA, EGTA, or vitamin E. Figure 7c evaluated that BAPTA-AM, EGTA, and vitamin E significantly attenuated the increase in hippocampal neurons with morphological alterations of nuclei by approximately 36.9%, 40.6%, and 42.8%, respectively. Single treatment with neither EGTA, BAPTA-AM, nor vitamin E altered the number of hippocampal neurons with apoptotic nuclei at 12 h (less than 5% of total neurons).

Discussion

Results presented here suggest that EGCG induced calcium overload in a concentration-dependent way in cultures of hippocampal neurons, the elevation intracellular $[Ca^{2+}]_i$ from both internal calcium stores of the endoplasmic reticulum (ER) and extracellular calcium influx leading to the deregulation of $[Ca^{2+}]_i$ homeostasis. EGCG exposure also caused an increase in ROS production and the collapse of mitochondrial membrane potential with concomitant alterations in the ratio of Bcl-2/Bax expression in a time-dependent manner. These results showed that EGCG may induce cell death in the primary hippocampal cultures. Cell death was also characterized by typical phosphatidylserine externalization (data not shown) and chromatin condensation. Based on these results, we supposed that the complex relationship between the elevation of $[Ca^{2+}]_i$ and mitochondrial function formed a foundation which leads to EGCG-induced hippocampal neuron death (Fig. 8). The neuron death relies on a balance between mitochondrial function and $[Ca^{2+}]_i$ homeostasis, and calcium overload induces an imbalance in mitochondrial homeostasis, leading to mitochondrial dysfunction, which eventually triggers neuronal death.

EGCG has been demonstrated to penetrate the plasma membrane readily by passive diffusion (Sugisawa and

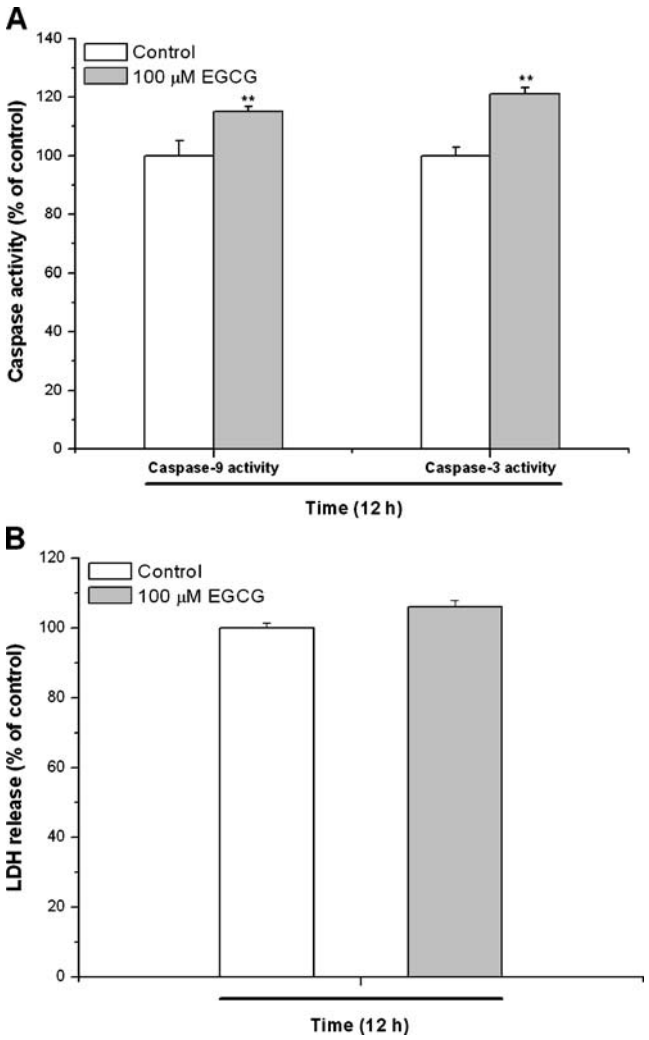

Fig. 6 **A** Caspase-9 and caspase-3 activities are increased after 100 μM EGCG exposure for 12 h compared with control. Caspase-9 and caspase-3 activation in cultures of hippocampal neurons was measured using the chromogenic substrate Ac-LEHD-*p*NA and Ac-DEVD-*p*NA. Each value was expressed as the ratio of caspase-9 or caspase-3 activation level to control level, and the value of control was set to 100%. **B** Percentage of cell death from necrosis as reflected by the amount of LDH release is not significantly increased up to 12 h after 100 μM EGCG exposure compared with control ($p>0.05$). Data are mean±SEM from at least six to nine wells from three independent experiments. $^{**}p<0.01$ compared to corresponding value in control cultures. One-way ANOVA with the Bonferroni post hoc test was used for statistical analysis

Umegaki 2002). Upon a 12-h exposure to EGCG, the hippocampal neurons developed cytoplasmic vacuoles that occasionally increased to balloon-like dimensions. Similar aberrations were reported in cells exposed to agents generating ROS (Babich et al. 1996). The involvement of cytoplasmic vacuoles in oxidative stress has received some attention (Zhang and Brunk 1993), particularly, as the Fenton reaction may occur within lysosomes.

An initial elevation in $[Ca^{2+}]_i$ is thought to be causative for subsequent cytotoxic processes, including ROS formation, mitochondrial injury, and ultimately cell death (Norenberg and Rao 2007). When mitochondria are exposed to high Ca^{2+} levels, Ca^{2+} uptake may interfere with mitochondrial function, leading to the activation of mitochondria permeability transition (mPT) and cell death pathways. For example, mitochondrial Ca^{2+} accumulation can lead to ROS formation, mitochondrial membrane depolarization, mPT activation, and a secondary increase in Ca^{2+} levels (Carriedo et al. 2000). As shown herein and by others, EGCG can act as a pro-oxidant (Raza and John 2005). Upon cell entry, EGCG generates ROS, which coincided with loss in $\Delta\psi_m$. The production of ROS is expected to induce adverse effects on many aspects of neuronal cell function. In particular, local damage impairs mitochondrial energy production, enhancing depletion of cellular energy stores and leading to the impairment of a myriad of homeostatic or protective mechanisms (Dugan et al. 1995). In addition, ROS production depletes cellular antioxidant defenses, leading to a more global enhancement of oxidative stress and free radical-mediated injury throughout the cell. It seems reasonable, therefore, that ROS production induced by EGCG is an event associated with calcium overload and subsequent mitochondrial dysfunction, which eventually is a critical event dictating the fate of neurons.

Oxidative stress has been implicated in mediating apoptosis induced by various toxicants (Yokoyama et al. 2007). Our results are, thus, in line with these observations. Oxidative stress may be involved in mediating apoptosis at early and/or late stages through different possible mechanisms (Fleury et al. 2002). In EGCG-exposed hippocampal neurons, increased ROS were observed 1 h post-exposure. This and the fact that the observed percentage of ROS positive was proportional to the EGCG exposure concentration and equal to the percentage of cells undergoing EGCG-induced apoptosis suggest that the EGCG-generated oxidative stress may be primarily involved in the early phase of apoptosis.

A pivotal role for mitochondrial membrane depolarization in apoptosis is suggested by several different observations (Guo et al. 1997). Our data indicate that EGCG causes a progressive decrease in mitochondrial transmembrane potential, as measured using the fluorescent probe JC-1, which occurs after 4 h of exposure to 100 μM EGCG. Calcium uptake and ROS production have been causally linked to mitochondrial membrane depolarization in cells undergoing apoptosis. In the present study, JC-1 fluorescence in EGCG-exposed hippocampal neurons clearly showed that EGCG increases oxidative activity in the cells and accounts for ROS generation, which leads to a decrease in $\Delta\psi_m$ and cell death. But the mechanisms by which ROS might increase loss in $\Delta\psi_m$ in EGCG-treated hippocampal neurons remain, however, unclear. One hypothesis would be that EGCG-induced ROS would have triggered mitochondrial membrane lipid peroxidation, leading to disruption of

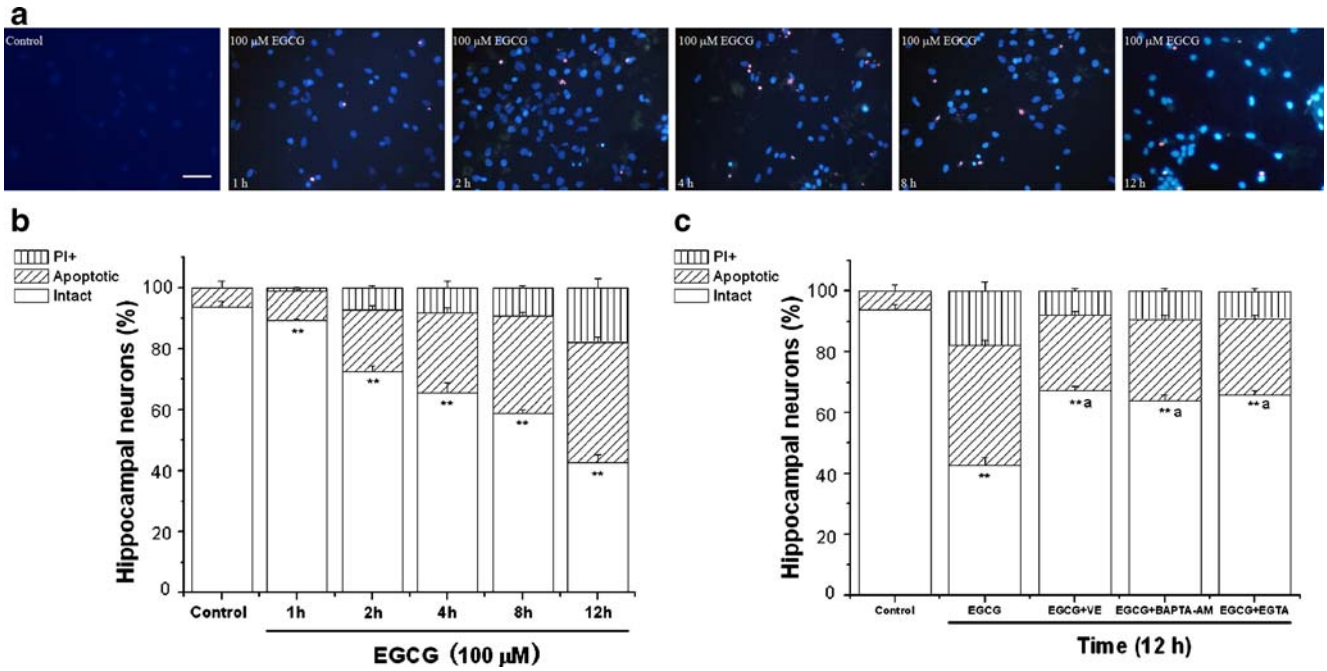

Fig. 7 Quantification of number of cultures of hippocampal neurons with nuclear alterations. Number of neurons treated with 100 μM EGCG for 1, 2, 4, 8, or 12 h with morphological alterations of nuclei was determined by using the fluorescent dye Hoechst 33342 and PI. **a** Representative photographs showing the nuclear morphology of hippocampal neurons in control and 100 μM EGCG exposed for 1, 2, 4, 8, or 12 h, respectively. **b** Time-course change caused by 100 μM EGCG. **c** Protective effect of 20 μM vitamin E, 5 μM BAPTA-AM, and 5 mM EGTA against neuronal damage induced by 100 μM EGCG treatment for 12 h. *Intact*, neurons with normal appearance of dark-blue Hoechst 33342-stained nucleus as well as absence of a red PI staining; *Apoptotic*, neurons with distinctively condensed and intensively blue-stained nuclei, but lacking PI staining; *PI+*, neurons with red PI staining (necrotic/late-stage apoptotic). Data are expressed as mean±SEM of five to ten random fields/culture determinations of four distinct experiments. $^{**}p<0.01$ vs. control group and "a" $p<0.01$ vs. 100 μM EGCG-treated group. One-way ANOVA with the Bonferroni post hoc test was used for statistical analysis. Scale bar in graphs 20 μm

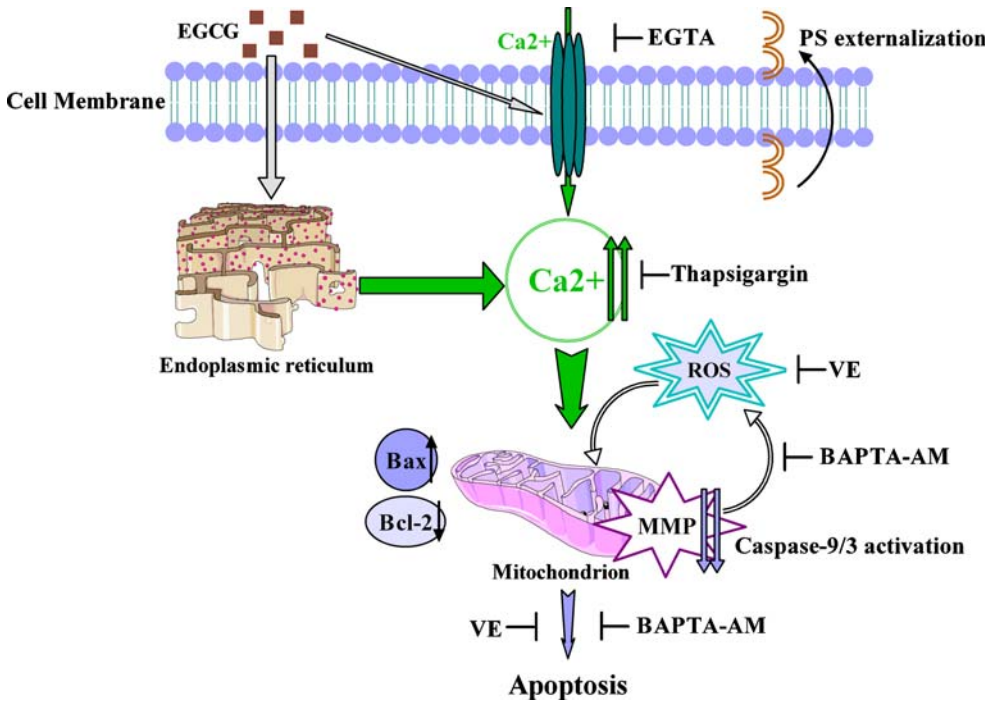

Fig. 8 Schematic summary of pathways involved in EGCG-induced cell death in cultures of hippocampal neurons

$\Delta\psi_m$. An alternative hypothesis would be that ROS might have altered expression of mitochondrial anti-apoptotic proteins.

The Bcl-2 family of anti-apoptotic proteins and pro-apoptotic proteins are important modulators in regulating cell death (Akhtar et al. 2004). In addition, altered ratio of pro- to anti-apoptotic Bcl-2 family proteins is significant in determining if apoptosis occurs. In our study, Western blot analysis revealed that compared with the control group, the Bcl-2/Bax ratio was decreased significantly by treatment with EGCG. Therefore, it can be speculated that the modulation of Bcl-2/Bax expression by EGCG might be an important factor in signal transduction mediating its toxic effect in hippocampal neurons. Furthermore, exposure of cultured hippocampal neurons to 100 μM EGCG was also shown to induce the elevation of caspase-3 and caspase-9 activity with no significant accompaniment of LDH release, thus providing further evidence that cell apoptosis was the prevailing type of EGCG-induced cell death in hippocampal neurons.

Findings of the pro-oxidant nature of EGCG appear to conflict with the generally recognized concept that tea polyphenolics, including EGCG, act as antioxidants (Saffari and Sadrzadeh 2004; Yao et al. 2008). The apparent contradiction in the biological activity of EGCG may reflect differences in experimental design, specifically the cell line. It has been suggested that the antioxidant activity of EGCG might be due to the radical scavenging activity of its flavin unit, whereas its pro-oxidant activity may be due to the flavonoids unit of catechin (Sakagami et al. 2001). However, the mechanism whereby EGCG changes from antioxidant activity to pro-oxidant activity, and vice versa, was uncertain.

Consumption of six or seven cups of green tea per day (corresponding to a dose of ~30 mg EGCG/kg per day) will result in a plasma EGCG concentration of approximately 1 μg/ml (approximately 2.2 μM; Yang et al. 1998). However, higher plasma EGCG concentrations can be achieved by taking EGCG supplements (Chow et al. 2001). It has also been reported that two doses, 24 h apart, of 50 mg EGCG/kg/day produced plasma EGCG levels up to 44 μg/ml (approximately 96 μM; Isbrucker et al. 2006). The concentration of 100 μM EGCG was also a concentration used widely in other studies in which EGCG act as antioxidant in cancer cells (Hwang et al. 2007). So the EGCG concentrations used in our study were determined by extrapolating from these previous reports. But further studies exploring in vitro/in vivo correlation and inter-species scaling would provide a more accurate estimation of concentrations/doses of EGCG and its effect in humans. Prediction of the dosage requirement for humans still requires accessible in vitro biological data and other absorption estimates obtained from in vitro animal models.

In summary, our data identify key events in a biochemical cascade induced by EGCG in cultures of hippocampal neurons. The results suggest that EGCG has a pro-oxidative effect on hippocampal neurons, and this seems to be directly associated with intracellular calcium overload, ROS generation, mitochondrial injury, caspase activation, and regulation of the Bcl-2 family (Fig. 8). The occurrence of these rate-limiting steps implicates the activation and involvement of the mitochondrial apoptotic pathway in mediating EGCG-induced cell death in hippocampal neurons. Our findings also point to the involvement of an oxidative stress-mediated mechanism in the execution of EGCG-induced cell death in hippocampal neurons.

Acknowledgments This work was supported by the National Nature Science Foundation of China (Nos. 30630057, 30670554, and 30670662) and Anhui High Education Natural Science Program (No. ZD2008010-2).

References

Akhtar RS, Ness JM, Roth KA (2004) Bcl-2 family regulation of neuronal development and neurodegeneration. Biochim Biophys Acta 1644:189–203

Babich H, Zuckerbraun HL, Wurzburger BJ, Rubin YL, Borenfreund E, Blau L (1996) Benzoyl peroxide cytotoxicity evaluated in vitro with the human keratinocyte cell line, RHEK-1. Toxicology 106:187–196

Bandele OJ, Osheroff N (2008) (−)-Epigallocatechin gallate, a major constituent of green tea, poisons human type II topoisomerases. Chem Res Toxicol 21:936–943

Berridge MJ, Lipp P, Bootman MD (2000) The versatility and universality of calcium signalling. Nat Rev Mol Cell Biol 1:11–21

Cafe C, Torri C, Bertorelli L, Tartara F, Tancioni F, Gaetani P, Rodriguez y, Baena R, Marzatico F (1995) Oxidative events in neuronal and glial cell-enriched fractions of rat cerebral cortex. Free Radic Biol Med 19:853–857

Carriedo SG, Sensi SL, Yin HZ, Weiss JH (2000) AMPA exposures induce mitochondrial Ca^{2+} overload and ROS generation in spinal motor neurons in vitro. J Neurosci 20:240–250

Chacon E, Acosta D (1991) Mitochondrial regulation of superoxide by Ca2+: an alternate mechanism for the cardiotoxicity of doxorubicin. Toxicol Appl Pharmacol 107:117–128

Choi D, Kim D, Park Y, Chun B, Choi S (2002) Protective effects of rilmenidine and AGN 192403 on oxidative cytotoxicity and mitochondrial inhibitor-induced cytotoxicity in astrocytes. Free Radic Biol Med 33:1321–1333

Chow H-HS, Cai Y, Alberts DS, Hakim I, Dorr R, Shahi F, Crowell JA, Yang CS, Hara Y (2001) Phase I pharmacokinetic study of tea polyphenols following single-dose administration of epigallocatechin gallate and polyphenon E. Cancer Epidemiol Biomarkers Prev 10:53–58

Chung F-L, Schwartz J, Herzog CR, Yang Y-M (2003) Tea and cancer prevention: studies in animals and humans. J Nutr 133:3268S–3274S

Doutheil J, Althausen S, Gissel C, Paschen W (1999) Activation of MYD116(gadd34) expression following transient forebrain ischemia of rat: implications for a role of disturbances of endoplasmic reticulum calcium homeostasis. Brain Res Mol Brain Res 63:225–232

Dugan L, Sensi S, Canzoniero L, Handran S, Rothman S, Lin T, Goldberg M, Choi D (1995) Mitochondrial production of reactive oxygen species in cortical neurons following exposure to *N*-methyl-D-aspartate. J Neurosci 15:6377–6388

Ermak G, Davies KJ (2002) Calcium and oxidative stress: from cell signaling to cell death. Mol Immunol 38:713–721

Fleury C, Mignotte B, Vayssière J-L (2002) Mitochondrial reactive oxygen species in cell death signaling. Biochimie 84:131–141

Guo Q, Sopher BL, Furukawa K, Pham DG, Robinson N, Martin GM, Mattson MP (1997) Alzheimer's presenilin mutation sensitizes neural cells to apoptosis induced by trophic factor withdrawal and amyloid-peptide: involvement of calcium and oxyradicals. J Neurosci 17:4212–4222

Hwang J-T, Ha J, Park I-J, Lee S-K, Baik HW, Kim YM, Park OJ (2007) Apoptotic effect of EGCG in HT-29 colon cancer cells via AMPK signal pathway. Cancer Lett 247:115–121

Isbrucker RA, Bausch J, Edwards JA, Wolz E (2006) Safety studies on epigallocatechin gallate (EGCG) preparations. Part 1: Genotoxicity. Food Chem Toxicol 44:626–635

Kanadzu M, Lu Y, Morimoto K (2006) Dual function of (−)-epigallocatechin gallate (EGCG) in healthy human lymphocytes. Cancer Lett 241:250–255

Lambert JD, Yang CS (2003) Mechanisms of cancer prevention by tea constituents. J Nutr 133:3262s–3267s

Lambert JD, Sang S, Yang CS (2007) Possible controversy over dietary polyphenols: benefits vs risks. Chem Res Toxicol 20:583–585

Lin HH, Li W-W, Lee Y-C, Chu S-T (2007) Apoptosis induced by uterine 24p3 protein in endometrial carcinoma cell line. Toxicology 234:203–215

Makar TK, Nedergaard M, Preuss A, Gelbard AS, Perumal AS, Cooper AJL (1994) Cooper, vitamin E, ascorbate, glutathione, glutathione disulfide and enzymes of glutathione metabolism in cultures of chick astrocytes and neurons: evidence that astrocytes play an important role in antioxidative process in the brain. J Neurochem 62:45–53

Marttila RJ, Roytta M, Lorentz H, Rinne UK (1988) Oxygen toxicity protecting enzymes in the human brain. J Neural Transm 74: 87–95

Mattson MP, Lovell MA, Furukawa K, Markesbery WR (1995) Neurotrophic factors attenuate glutamate-induced accumulation of peroxides, elevation of $[Ca^{2+}]_i$ and neurotoxicity, and increase antioxidant enzyme activities in hippocampal neurons. J Neurochem 65:1740–1751

Nakagawa T, Yokozawa T (2002) Direct scavenging of nitric oxide and superoxide by green tea. Food Chem Toxicol 40:1745–1750

Nicotera P, Zhivotovsky B, Orrenius S (1994) Nuclear calcium transport and the role of calcium in apoptosis. Cell Calcium 16: 279–288

Norenberg MD, Rao KVR (2007) The mitochondrial permeability transition in neurologic disease. Neurochem Int 50:983–997

Park HJ, Shin D-H, Chung WJ, Leem K, Yoon SH, Hong MS, Chung J-H, Bae J-H, Hwang JS (2006) Epigallocatechin gallate reduces hypoxia-induced apoptosis in human hepatoma cells. Life Sci 78:2826–2832

Raza H, John A (2005) Green tea polyphenol epigallocatechin-3-gallate differentially modulates oxidative stress in PC12 cell compartments. Toxicol Appl Pharmacol 207:212–220

Reyes-Martin P, Alique M, Parra T, JPd Hornedo, Lucio-Cazana J (2007) Cyclooxygenase-independent inhibition of H_2O_2-induced cell death by S-ketoprofen in renal cells. Pharmacol Res 55: 295–302

Saffari Y, Sadrzadeh SMH (2004) Green tea metabolite EGCG protects membranes against oxidative damage in vitro. Life Sci 74:1513–1518

Sai K, Kai S, Umemura T, Tanimura A, Hasegawa R, Inoue T, Kurokawa Y (1998) Protective effects of green tea on hepatotoxicity, oxidative DNA damage and cell proliferation in the rat liver induced by repeated oral administration of 2-nitropropane. Food Chem Toxicol 36:1043–1051

Sakagami H, Arakawa H, Maeda M, Satoh K, Kadofuku T, Fukuchi K, Gomi K (2001) Production of hydrogen peroxide and methionine sulfoxide by epigallocatechin gallate and antioxidants. Anticancer Res 21:2633–2641

Schmidt M, Schmitz HJ, Baumgart A, Guedon D, Netsch MI, Kreuter MH, Schmidlin CB, Schrenk D (2005) Toxicity of green tea extracts and their constituents in rat hepatocytes in primary culture. Food Chem Toxicol 43:307–314

Sugisawa A, Umegaki K (2002) Physiological concentrations of (−)-epigallocatechin-3-*O*-gallate (EGCg) prevent chromosomal damage induced by reactive oxygen species in WIL2-NS cells. J Nutr 132:1836–1839

Sunanda, Rao BS, Raju TR (1998) Corticosterone attenuates zinc-induced neurotoxicity in primary hippocampal cultures. Brain Res 791:295–298

Yang CS, Chen L, Lee M-J, Balentine D, Kuo MC, Schantz SP (1998) Blood and urine levels of tea catechins after ingestion of different amounts of green tea by human volunteers. Cancer Epidemiol Biomarkers Prev 7:351–354

Yao K, Ye P, Zhang L, Tan J, Tang X, Zhang Y (2008) Epigallocatechin gallate protects against oxidative stress-induced mitochondria-dependent apoptosis in human lens epithelial cells. Mol Vis 14:217–223

Yin ST, Tang ML, Su L, Chen L, Hu P, Wang HL, Wang M, Ruan DY (2008) Effects of epigallocatechin-3-gallate on lead-induced oxidative damage. Toxicology 249:45–54

Yokoyama Y, Nohara K, Okubo T, Kano I, Akagawa K, Kano K (2007) Generation of reactive oxygen species is an early event in dolichyl phosphate-induced apoptosis. J Cell Biochem 100:349–361

Zhang H, Brunk UT (1993) Alloxan cytotoxicity is highly potentiated by plasma membrane- and lysosomal-associated iron—a study on a model system of cultured J-774 cells. Diabetologia 36:707–715